

# Determination of contact and intrinsic nanowire resistivity in two-contact ZnO nanowire devices

Y. F. Lin<sup>1</sup>, W. B. Jian<sup>1</sup>, Z. Y. Wu<sup>2</sup>, F. R. Chen<sup>2</sup>, J. J. Kai<sup>2</sup>, J. J. Lin<sup>1,3</sup>

<sup>1</sup>Department of Electrophysics, National Chiao Tung University, Hsinchu 30010, China

<sup>2</sup>Department of Engineering and System Science, National Tsing Hua University, Hsinchu 30013, China

<sup>3</sup>Institute of Physics, National Chiao Tung University, Hsinchu 30010, China

**Abstract**—Cylindrical ZnO nanowires were synthesized to fabricate two-contact ZnO nanowire devices with the same separation distance between the two contact electrodes. Electrical properties including temperature dependence of resistance and  $I$ - $V$  curves were recorded. According to distinct electrical behaviors and room-temperature resistance, ZnO nanowire devices can be categorized into three different types exhibiting either contact or intrinsic NW attributes.

## I. INTRODUCTION

The advance in nanostructure synthesis with the employment of electron microscopy for atomic-range structure characterization [1] facilitates to explore fundamental physics and to discover rich and unique properties on the nano scale. Among all the nanostructures, quasi-one-dimensional materials, such as nanowires and nanobelts, are the best candidates to make basic building blocks of nanoscale devices for electric, optoelectronic, and bioengineering applications [2-4], so as to substitute the bottom-up fabrication technology for the top-down production way. In order to build feasible and practical nanowire devices, exploring electrical properties of individual nanowires (NWs) has received particular attention.

Research on ZnO materials started in 1930s [5] and gradually declined after 1980s due possibly to difficulties in doping this material in  $p$ -type manner and in regulating oxygen nonstoichiometry. Because of the capabilities of room-temperature lasing and of forming ferromagnetic oxide with doped  $3d$ -transition elements, ZnO has aroused concentration recently. By using ZnO NWs, the applications of chemical sensors [6], gas sensors [7], UV light sensors [8], field effect transistors [9], Schottky diodes [10], and piezoelectric power generators [11] have been demonstrated latterly. Among previously presented ZnO NW device, most of them were lithographically patterned to carry two contact electrodes. Since rectifying Schottky contacts exist inevitably between metal and semiconductor interface, intrinsic current-voltage ( $I$ - $V$ ) behaviors of individual ZnO NWs cannot be effortlessly obtained from those two-contact NW devices [12]. In fact, the  $I$ - $V$  curves of these ZnO NW devices display linear (Ohmic), rectifying (Schottky diode), upward-bending, or downward-bending features. On the other hand, electron transport in ZnO NW devices can be depicted and understood through temperature dependences of  $I$ - $V$  curves and electrical resistances. Heo *et al.* [13] reported the thermal activated transport in ZnO NWs and acquired

activation energy of  $\sim 90$  meV which could not be ascribed to any known ionization energy of native donor defects in ZnO. Ma *et al.* [14] suggested the model of Efros-Shklovskii variable range hopping to explain the temperature dependent resistance of their two-contact ZnO NW devices. A comprehending determination of electron transport in either contacts or ZnO NWs is still lacking.

In this work, we conducted a series of systematic experiments to inquire into  $I$ - $V$  characteristics and electron transport in either electro-contacts or NWs of the two-contact ZnO NW devices. More than thirty devices were fabricated for electrical-property investigation. According to their room-temperature (RT) resistances and  $I$ - $V$  behaviors, the two-contact ZnO NW devices can be categorized into three types to show both contact and intrinsic NW attributes.

## II. EXPERIMENTAL METHOD

Single-crystalline ZnO NWs with a cylindrical cross section and 40 nm in diameter were synthesized by vapor transport and structurally characterized by electron microscopy [15]. Micron leads, electro-pads, and alignment marks were patterned on silicon substrates which were capped with a 400-nm thick SiO<sub>2</sub> layer. ZnO NWs were then randomly dispersed on substrates and positioned by using field-emission scanning electron microscope (FESEM, JEOL JSM-7000F). The Ti/Au (20/100-nm thickness) double-layer leads were deposited by using standard e-beam lithography and thermal evaporation, to connect the NWs with micron current leads. A schematic diagram of our two-contact ZnO NW devices is given in Fig. 1. The separation distance of  $\sim 1\mu\text{m}$  between two Ti/Au leads was kept the same for all devices. Afterwards, the ZnO NW devices were placed in a liquid-nitrogen cryostat and  $I$ - $V$  curves at various temperatures were recorded.

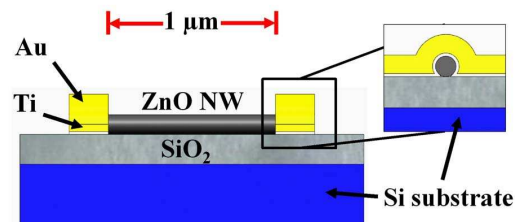


Fig. 1. A schematic illustration of a ZnO NW device. The separation distance between the two contact electrodes is about  $1\mu\text{m}$ .

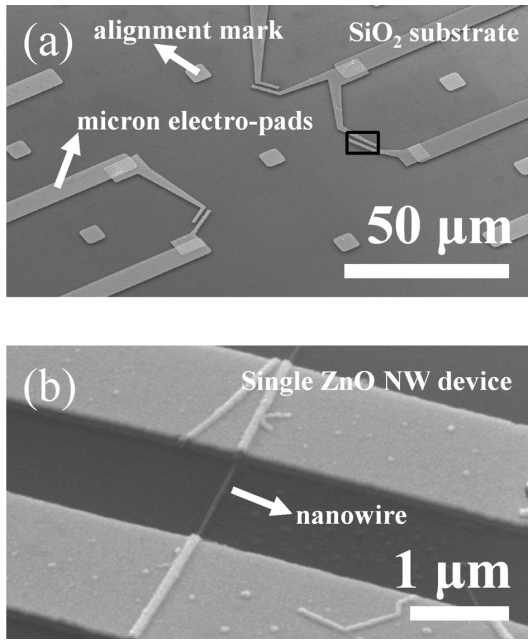


Fig. 2. (a) FESEM image of a typical nanowire device with pre-fabricated micron electro-pads and alignment marks. An image of the indicated rectangular area is given in (b). This high-resolution FESEM image displays a close view of a single ZnO NW under two Ti/Au electrodes.

### III. RESULT AND DISCUSSION

FESEM image of a typical single ZnO NW device is presented in Fig. 2(a) and the high-resolution FESEM image of the indicated rectangular area (in Fig. 2(a)) is given in Fig. 2(b). The alignment marks are used for the e-beam writer to determine the position of our randomly dispersed ZnO NWs. Although the separation distance between current leads is kept the same, the NW devices displayed extremely variant RT resistance and different attributes in  $I$ - $V$  curves. We therefore categorized all the ZnO NW devices into three types.

Figure 3 shows electrical behaviors of the first type (Type I) of single ZnO NW devices. Since the RT resistance was about two orders of magnitude larger, as compared with other types of NW devices, the back-to-back Schottky diode model was adopted to analyze the electrical behaviors. The general Schottky and thermionic emission theory can be described in the following expressions [16]:

$$I = I_{ST} \exp\left(\frac{qV}{nk_B T}\right) \left[1 - \exp\left(-\frac{qV}{k_B T}\right)\right], \quad (1)$$

$$I_{ST} = SA^* T^2 \exp\left(-\frac{q\Phi_{BE}}{nk_B T}\right), \quad (2)$$

where  $T$  is the temperature,  $k_B$  is the Boltzmann constant,  $I_{ST}$  is the saturation current,  $n$  is the ideality factor,  $S$  is the contact area,  $A^*$  is the Richardson constant, and  $q\Phi_{BE}$  is the effective barrier height. Type I devices evidenced a high RT resistance and an upward bending feature in  $I$ - $V$  curves as shown in Fig.

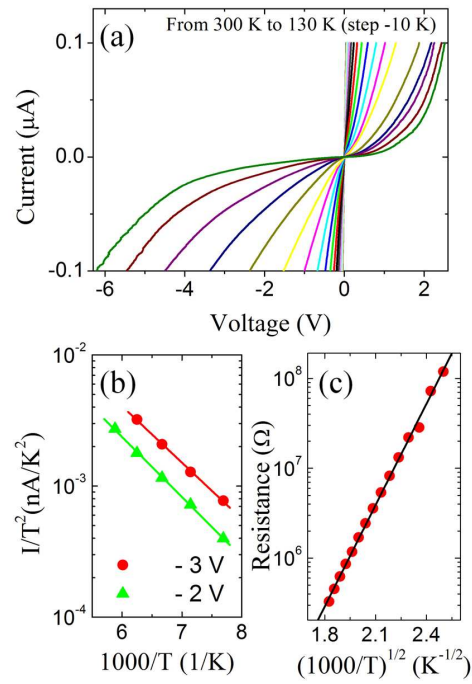


Fig. 3. (a) Temperature dependent  $I$ - $V$  curves of a Type I ZnO NW device with a high RT resistance of  $\sim 0.5$  M $\Omega$ . (b)  $\ln(I/T^2)$  as a function of  $T^{-1}$  at  $-2$  and  $-3$  V. (c)  $\ln R$  as a function of  $T^{-1/2}$  from 130 to 300 K.

3(a). The upward bending feature implies a rapidly increasing current in the breakdown voltage range. Figure 3(b) reveals a temperature dependence of  $\ln(I/T^2)$  which is in conformity with Eq. (2) and the effective Schottky barrier of  $\sim 100$  meV can be estimated.

Since the resistance of Type I devices mainly comes from the electro-contacts, electron transport in contacts might be disclosed through measuring the temperature dependent resistance. Figure 3(c) offers a linear  $T^{-1/2}$  dependence of  $\ln R$  which is in line with the variable range hopping theory of the form [17]:

$$R = A \exp(BT^{-1/2}), \quad (3)$$

where  $R$  is the resistance, and  $A$  and  $B$  are constants. The electron transport of Type I devices suggests the electron hopping model in the disordered medium at interfaces between metal and semiconductor. The disordered medium could possibly result from oxidized Ti electrodes or from the non-crystalline outermost layer on surfaces of ZnO NWs.

Figure 4 unveils characteristics of a Type II ZnO NW device which possesses a low RT resistance of  $\sim 15$  k $\Omega$ . The  $I$ - $V$  curves (see Fig. 4(a)) delineate a linear dependence within the low voltage range (from  $-40$  to  $40$  mV) that proclaims Ohmic contacts between Ti/Au metal leads and ZnO NWs for our Type II devices. On the other hand, owing to the Ohmic and low-resistance contacts, Type II devices provides for determination of intrinsic NW resistivity. Figure 4(b) shows the temperature dependent resistance being in line with the

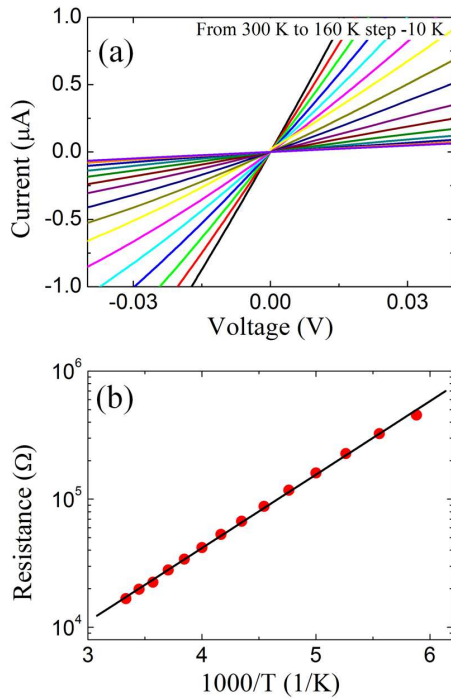


Fig. 4. (a)  $I$ - $V$  curves at various temperatures of a Type II ZnO NW device with a RT resistance of  $\sim 15$  k $\Omega$ . (b)  $\ln(R)$  as a function of  $T^{-1}$  with the best fitting line.

thermally activated transport of the form [18]:

$$R \propto \exp\left(\frac{\Delta E_a}{2k_B T}\right), \quad (4)$$

where  $\Delta E_a$  is the activation energy. The temperature behavior coincided properly with semiconductor transport in ZnO NWs and the activation energy was evaluated to be  $\sim 200$  meV by linear least-square fitting. In this case, the activation energy of natively  $n$ -type dopants cannot be assigned to any of known shallow donor levels [13, 19, 20] in ZnO. The calculated activation energy is justly in consistency with the value obtained from our four-contact measurements. Type II ZnO NW devices provide an estimate of intrinsic NW resistivity if the contact resistance is neglected. The intrinsic ZnO NW resistivity was found to be about several m $\Omega$ -cm and, in the mean time, it was confirmed by using our four-contact NW devices.

Besides Type I and II devices, there is still a third type (Type III) of ZnO NW devices and it demonstrates a manner of rectifying  $I$ - $V$  curves as shown in Fig. 5. The rectifying attribute is more pronounced at a lower temperature. Type III ZnO NW devices can be modeled as one-side Ohmic and one-side Schottky contacts. The voltage and temperature dependent currents are able to be interpreted by thermionic emission theory (see Eq. (1) and (2)). For the 200-K  $I$ - $V$  curve, it must be noted that, the on and off ratio (between -0.2 and 0.2 V) of the rectifying character is about 125. The inset in Fig. 5 exposes an exact fitting to Eq. (1) in a very wide

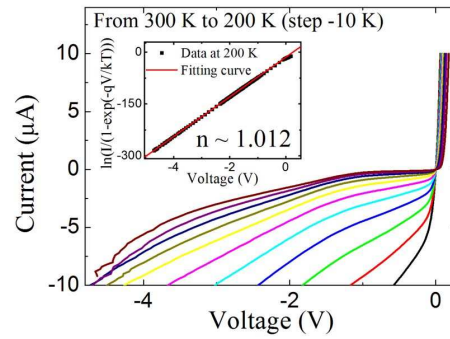


Fig. 5  $I$ - $V$  curves of a Type III ZnO NW device with a RT resistance of  $\sim 50$  k $\Omega$ . The inset shows a precisely good fitting to thermionic emission theory in a wide voltage range.

voltage range. The ideality factor is computed to be 1.0 which sustains exclusively our explanation by using one-side Ohmic and one-side Schottky contact model. Type III ZnO NW devices, which manifest themselves in a character of a rectifying  $I$ - $V$  performance, occur in an exceptionally broad RT resistance range.

### III. CONCLUSION

More than thirty ZnO NW devices were fabricated for performing temperature dependent  $I$ - $V$  curves and resistance measurements. The NW devices were categorized into three types (Type I-III) in compliance with electrical behaviors and RT resistances. Type I devices revealed a high RT resistance, a downward bending trend on  $I$ - $V$  graphs, and a linear dependence on  $\ln R$  versus  $T^{-1/2}$  graphs. We suggested that Type I devices could be modeled as back-to-back Schottky diode and their temperature dependent resistance could be elucidated through the model of electron's variable range hopping in contacts. Type II devices, being modeled as two Ohmic contacts, uncover the intrinsic resistivity ( $\sim$ several m $\Omega$ -cm) of individual ZnO NWs. For the Type III devices, their RT resistances cover a thoroughly broad range and they present Schottky rectifying attributes on  $I$ - $V$  graphs. Additionally and surprisingly, their variant current could be fitted precisely and coincidentally with thermionic emission theory in a wide voltage range. As a consequence, we have accurately determined electrical properties of both contacts and ZnO NWs by employing the two-contact ZnO NW devices.

### ACKNOWLEDGMENT

This work was supported by the Taiwan National Science Council under Grant Nos. NSC 94-2112-M-009-020 and NSC 95-2120-M-009-002, and by the MOE ATU Program.

### REFERENCES

- [1] Y. Ding and Z. L. Wang, "Structure analysis of nanowires and nanobelts by transmission electron microscopy," *J. Phys. Chem. B*, vol. 108, pp. 12280-12291, July 2004.
- [2] X. Duan, Y. Huang, Y. Cui, J. Wang, and C. M. Lieber, "Indium phosphide nanowires as building blocks for nanoscale electronic and optoelectronic devices," *Nature*, vol. 409, pp. 66-69, January 2001.
- [3] Y. Cui, Q. Wei, H. Park, and C. M. Lieber, "Nanowire nanosensors

- for highly sensitive and selective detection of biological and chemical species," *Science*, vol. 293, pp. 1289-1292, August 2001.
- [4] X. Younan et al., "One-dimensional nanostructures: synthesis, characterization, and application," *Adv. Mater.*, vol. 15, pp. 353-389, March 2003.
- [5] C. Kilngshim, "ZnO: material, physics and applications," *ChemPhysChem*, vol. 8, pp. 783-803, 2007.
- [6] Q. Wan et al., "Fabrication and ethanol sensing characteristics of ZnO nanowire gas sensors," *Appl. Phys. Lett.*, vol. 84, pp. 3654-3656, May 2004.
- [7] Q. H. Li, Y. X. Liang, Q. Wan, and T. H. Wang, "Oxygen sensing characteristics of individual ZnO nanowire transistors," *Appl. Phys. Lett.*, vol. 85, pp. 6389-6391, December 2004.
- [8] M. H. Huang, Y. Wu, H. Feick, N. Tran, E. Weber, and P. Yang, "Catalytic growth of Zinc oxide nanowires by vapor transport," *Adv. Mater.*, vol. 13, pp. 113-116, January 2001.
- [9] Z. Fan, D. Wang, P. C. Chang, W. Y. Tseng, and J. G. Lu, "ZnO nanowire field-effect transistor and oxygen sensing property," *Appl. Phys. Lett.*, vol. 85, pp. 5923-5925, December 2004.
- [10] Y. W. Heo et al., "Pt/ZnO nanowire Schottky diodes," *Appl. Phys. Lett.*, vol. 85, pp. 3107-3109, October 2004.
- [11] J. Song, J. Zhou, and Z. L. Wang, "Coupled power generating process of a single ZnO belt/wire. A technology for harvesting electricity from the environment," *Nano Lett.*, vol. 6, pp. 1656-1662, 2006.
- [12] W. Gu, H. Choi, and K. K. Kim, "Universal approach to accurate resistivity measurement for a single nanowire: theory and application," *Appl. Phys. Lett.*, vol. 89, pp. 253102-1-3, 2006.
- [13] Y. W. Heo et al., "Electrical transport properties of single ZnO nanorods," *Appl. Phys. Lett.*, vol. 85, pp. 2002-2004, September 2004.
- [14] Y. J. Ma., "Hopping conduction in single ZnO nanowires," *Nanotechnology*, vol. 16, pp. 746-749, April 2005.
- [15] Z. Y. Wu, F. R. Chen, W. B. Jian, and J. J. Lin, "Fabrication, characterization and studies of annealing effects on ferromagnetism in ZnO<sub>1-x</sub>Co<sub>x</sub>O nanowires," *Nanotechnol.*, vol. 17, pp. 5511-5518, October 2006.
- [16] S. M. Sze, and K. K. NG, *Physics of Semiconductor Devices*, 3<sup>rd</sup> ed., Wiley, New York, 2007, pp 154-157.
- [17] N. F. Mott, E. A. Davis, *Electronic Processes in Non-Crystalline Materials*, Oxford, Clarendon, 1979, pp 32-34.
- [18] S. M. Sze, and K. K. NG, *Physics of Semiconductor Devices*, 3<sup>rd</sup> ed., Wiley, New York, 2007, pp 21-25.
- [19] D. C. Look et al., "Evidence for native-defect donors in n-type ZnO," *Phys. Rev. Lett.*, vol. 95, pp. 225502-1-4, November 2005.
- [20] A. Tsukazaki, A. Ohtomo, M. Kawasaki, "High-mobility electronic transport in ZnO thin films," *Appl. Phys. Lett.*, vol. 88, pp. 152106-1-3, 2006.